



## Chemical reaction effect on peristaltic motion of micropolar fluid through a porous medium with heat absorption in the presence of magnetic field

R. N. Barik<sup>a</sup> and G. C. Dash<sup>b</sup>

<sup>a</sup>Department of Mathematics, Trident Academy of Technology, Infocity Area, Bhubaneswar, Odisha, India

<sup>b</sup>Department of Mathematics, S. O. A. University, Bhubaneswar, Odisha, India

---

### ABSTRACT

An attempt is made to study the peristaltic motion of incompressible micropolar fluid through a porous medium in a two-dimensional symmetric channel. The effects of heat absorption and chemical reaction in the presence of magnetic field have been reported. This phenomenon is modulated mathematically by a system of partial differential equations which govern the motion of the fluid. The flow analysis has been developed for low Reynolds number and long wavelength case. The expressions of the stream function, velocity, microrotation velocity, temperature and concentration are obtained as functions of the physical parameters of the problem. The results have been discussed graphically to observe the effects of heat absorption, chemical reaction and magnetic field in the presence of micropolarity effects through a set of figures. It is found that both the linear velocity and microrotation velocity decrease with increasing values of the micropolar fluid material parameter ( $m$ ). The effect of increasing the values of porosity parameter and magnetic parameter is to suppress microrotation velocity and enhance the linear velocity. It is also observed that an increase in the values of the coefficient of heat absorption parameter decreases the temperature field and increases the concentration field.

**Key words:** Peristaltic motion, Micropolar fluid, Porous medium, Chemical reaction, Symmetric flow.

---

### INTRODUCTION

Peristaltic motion is a phenomenon that occurs when expansion and contraction of an extensible tube in a fluid generate progressive waves which propagate along the length of the tube, mixing and transporting the fluid in the direction of wave propagation. It is an inherent property of many tubular organs of the human body. In some biomedical instruments, such as heart-lung machines, peristaltic motion is used to pump blood and other biological fluids. Peristaltic pumping is a form of fluid transport generally from a region of lower to higher pressure, by means of a progressive wave of area contraction or expansion, which propagates along the length of a tube like structure. Some electrochemical reactions are held responsible for this phenomenon. This mechanism occurs in swallowing of food through esophagus, in the ureter, the gastro intestinal tract, the bile duct, and even in small blood vessels. It has now been accepted that most of the physiological fluids behave like a non-Newtonian fluids. The peristaltic flows have attracted a number of researchers because of wide applications in physiology and industry.

The study of heat and mass transfer for an electrically conducting micropolar fluid past a porous plate under the influence of a magnetic field has attracted the interest of many investigators in view of its applications in many engineering problems such as magnetohydrodynamic (MHD) generators, plasma studies, nuclear reactors, oil exploration, geothermal energy extractions, and the boundary layer control in the field of aerodynamics.

The combined heat and mass transfer problems with chemical reactions are of importance in many processes and, therefore, have received a considerable amount of attention in recent years. In processes, such as drying, evaporation at the surface of a water body, energy transfer in a wet cooling tower, and the flow in a desert cooler, the heat and mass transfer occurs simultaneously.

Convection problems associated with heat sources within fluid-saturated porous media are of great practical significance, for that there are a number of practical applications in geophysics and energy-related problems, such as recovery of petroleum resources, geophysical flows, cooling of underground electric cables, storage of nuclear waste materials groundwater pollution, fiber and granular insulations, solidification of casting, chemical catalytic reactors, and environmental impact of buried heat generating waste.

Due to complexity of fluids, several models have been proposed in the literature. Amongst the several models of real fluids, the simplest one is the Newtonian. Equations which govern the flow of Newtonian fluids are the Navier–Stokes equations. But there are many fluids whose behavior cannot be described by the classical Navier–Stokes model. The inadequacy of the theory of Newtonian fluids in predicting the behavior of some fluids, especially those of high molecular weight leads to the development of non-Newtonian fluid mechanics. Undoubtedly, the governing equations for non-Newtonian fluids are of higher order, much more complicated and subtle in comparison with Newtonian fluids.

In some biomedical instruments, such as heart-lung machines, peristaltic motion is used to pump blood and other biological fluids. It plays an indispensable role in transporting many physiological fluids in the body in various situations such as (i) urine transport from the kidney to the bladder through the ureter, (ii) transport of spermatozoa in the ductus efferentes of the male reproductive tract, (iii) movement of ovum in the fallopian tubes, (iv) vasomotion of small blood vessels, (v) mixing and transporting the contents of the gastrointestinal passage, and so forth. Peristaltic pumping mechanisms have been utilised for the transport of slurries, sensitive or corrosive fluids, sanitary fluid, noxious fluids in the nuclear industry, to name but a few examples. It is well-known that many physiological fluids behave in general like suspensions of deformable or rigid particles in a Newtonian fluid. Blood, for example, is a suspension of red cells, white cells and platelets in plasma. Another example is cervical mucus, which is a suspension of macromolecules in a water-like liquid. In view of this, some researchers have tried to account for the suspension behaviour of biofluids by considering them to be non-Newtonian.

Past five decades considerable attention has been focused on the peristaltic transport of Newtonian and non-Newtonian fluids through tubes/channels. Such flows are significant in both theoretical and industrial perspectives. Peristaltic transport widely occurs in many biological systems for example, food swallowing through the esophagus, intra-urine fluid motion, circulation of blood in small blood vessels and the flows of many other glandular ducts. Several theoretical and experimental studies have been undertaken to understand peristalsis through abrupt changes in geometry and realistic assumptions. Kavitha et al. [1] investigated peristaltic flow of a micropolar fluid in a vertical channel with long wavelength approximation. Peristaltic motion of micropolar fluid in circular cylindrical tubes: effect of wall properties has been done by Muthu et al. [2]. Sreenadh et al. [3] reported the peristaltic flow of micropolar fluid in an asymmetric channel with permeable walls. On the influence of wall properties in the peristaltic motion of micropolar fluid are introduced by Muthu et al. [4]. Mekheimer [5] studied the non-linear peristaltic transport of magnetohydrodynamic flow in an inclined planar channel.

Elshehawey et al.[6] investigated the peristaltic transport in an asymmetric channel through a porous medium. Elmaboud [7] discussed the thermomicropolar fluid flow in a porous channel with peristalsis. El-dabe et al. [8] reported the heat absorption and chemical reaction effects on peristaltic motion of micropolar fluid through a porous medium in the presence of magnetic field. Muthu et al. [9] studied the peristaltic motion of micropolar fluid in circular cylindrical tubes: effect of wall properties. Reddy et al.[10] studied the peristaltic transport of a conducting fluid in an inclined asymmetric channel. Ali and Hayat [11] have investigated the peristaltic flow of a micropolar fluid in an asymmetric channel. Muthu et al. [12] have focused the peristaltic motion of micropolar fluid in circular cylindrical tubes: effect of wall properties. Sreenadh et al. [13] studied the peristaltic flow of micropolar fluid in an asymmetric channel with permeable walls. Harish Babu and Satya Narayan [14] have investigated the influence of variable permeability and radiation absorption on heat and mass transfer in MHD micropolar flow over a vertical moving porous plate. Hayat et al. [15] have studied a mathematical model of peristalsis in tubes through a porous medium. Mishra and Rao [16] discussed the peristaltic transport of a Newtonian fluid in an asymmetric channel.

Hemadri Reddy et al. [17] deal with the peristaltic pumping of a micropolar fluid in an inclined channel. Effect of magnetic field and wall properties on peristaltic motion of micropolar fluid has been discussed by Afifi et al. [18]. Peristaltic flow of a Newtonian fluid through a porous medium in a vertical tube under the effect of magnetic field has been studied by Vasudev et al. [19]. The effects of chemical reaction, heat and mass transfer on non-Newtonian fluid flow through porous medium in a vertical peristaltic tube has been discussed by El-Sayed et al. [20]. Peristaltic flow of a Prandtl fluid in a symmetric channel under the effect of a magnetic field has been studied by Jothi et al. [21]. Akbar et al. [22] have discussed the peristaltic flow of a Prandtl fluid in an asymmetric channel. Pandey and Chaube [23] have investigated the effect of magnetic field on the peristaltic flow of a micropolar fluid through a porous medium in a channel.

Recently, the peristaltic motion of non-Newtonian fluid with heat and mass transfer through a porous medium in channel under uniform magnetic field has been studied by Eldabe et al. [24]. Eldabe and Mohamed [25] studied the magnetohydrodynamic peristaltic flow with heat and mass transfer of micropolar biviscosity fluid through a porous medium between two co-axial tubes.

The objective of the present study is to consider the peristaltic motion of an incompressible micropolar fluid through a porous medium in a symmetric channel under the effects of heat absorption and chemical reaction in the presence of magnetic field with the assumption of long wavelength and low Reynolds number. The expressions of stream function, velocity, microrotation velocity, temperature and concentration are obtained. The effects of the fluid parameters on velocity, microrotation velocity, temperature and concentration have been studied with the help of graphs.

#### MATHEMATICAL FORMULATION

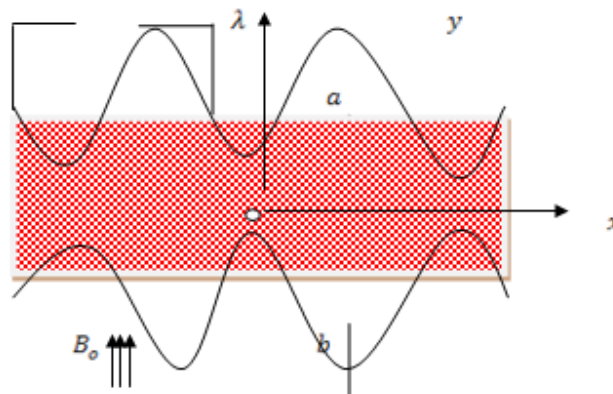


Fig. (1). Geometry of peristaltic transport of micropolar fluid through porous medium in a symmetric channel

The symmetric flow of an incompressible micropolar fluid through a porous medium in a symmetric channel has been considered. The flow is generated by sinusoidal wave propagating with constant speed  $c$  along the wall. A uniform magnetic field  $B_0$  is applied in the transverse direction of the flow. In the analysis, the cartesian coordinates  $(x, y)$  are taken, where  $x$  is along the channel and  $y$  is perpendicular to it as shown in fig.1.

The wall deformation is given by:

$$H = a + b \sin\left(\frac{2\pi}{\lambda}(x - ct)\right) \quad (1)$$

where  $a$  is the half width of the channel,  $b$  is the amplitude of the wave,  $\lambda$  is the wavelength and  $t$  is the time. The equations governing the two-dimensional transport of incompressible micropolar fluid through a porous medium in vertical channel under the effect of magnetic field are:

$$\frac{\partial u}{\partial x} + \frac{\partial v}{\partial y} = 0 \quad (2)$$

$$\rho \left[ u \frac{\partial u}{\partial x} + v \frac{\partial u}{\partial y} \right] = -\frac{\partial P}{\partial x} + k \frac{\partial \Omega}{\partial y} + (k + \mu) \left[ \frac{\partial^2 u}{\partial x^2} + \frac{\partial^2 u}{\partial y^2} \right] - \left( \frac{\mu}{k_i} + \sigma B_0^2 \right) u \quad (3)$$

$$\rho \left[ u \frac{\partial v}{\partial x} + v \frac{\partial v}{\partial y} \right] = -\frac{\partial P}{\partial y} + k \frac{\partial \Omega}{\partial x} + (k + \mu) \left[ \frac{\partial^2 v}{\partial x^2} + \frac{\partial^2 v}{\partial y^2} \right] - \frac{\mu}{k_i} v \quad (4)$$

$$\rho J \left[ u \frac{\partial \Omega}{\partial x} + v \frac{\partial \Omega}{\partial y} \right] - 2k\Omega + k \left[ \frac{\partial v}{\partial x} - \frac{\partial u}{\partial y} \right] + \gamma_1 \left[ \frac{\partial^2 \Omega}{\partial x^2} + \frac{\partial^2 \Omega}{\partial y^2} \right] \quad (5)$$

$$\rho C_p \left[ u \frac{\partial T}{\partial x} + v \frac{\partial T}{\partial y} \right] = k_r \left[ \frac{\partial^2 T}{\partial x^2} + \frac{\partial^2 T}{\partial y^2} \right] - Q_0 (T - T_0) \quad (6)$$

$$\left[ u \frac{\partial \phi}{\partial x} + v \frac{\partial \phi}{\partial y} \right] = D_m \left[ \frac{\partial^2 \phi}{\partial x^2} + \frac{\partial^2 \phi}{\partial y^2} \right] + \frac{D_m k_r}{T_m} \left[ \frac{\partial^2 T}{\partial x^2} + \frac{\partial^2 T}{\partial y^2} \right] - k_2 (\phi - \phi_0) \quad (7)$$

where  $u$  and  $v$  are velocity component,  $\rho$  is the density of the fluid,  $P$  is the pressure,  $k$  is the micropolar viscosity,  $\Omega$  is the microrotation velocity,  $\mu$  is the viscosity,  $k_i$  is the permeability of porous medium,  $\sigma$  is the conductivity of the fluid,  $J$  is the microinertia constant,  $\gamma_1$  is material constant,  $c_p$  is the specific heat,  $k_r$  is the thermal conductivity,  $T_m$  is the mean fluid temperature,  $D_m$  is the coefficient of mass diffusivity,  $Q_0$  is the heat absorption coefficient and  $k_2$  is the chemical reaction parameter.

Now, introduce the following non dimensional quantities as:

$$x^* = \frac{x}{\lambda}, y^* = \frac{y}{a}, h = \frac{H}{a}, t^* = \frac{tc}{\lambda}, u^* = \frac{u}{c}, v^* = \frac{v}{c\delta}, \delta = \frac{a}{\lambda}, P^* = \frac{Pa^2}{\mu\lambda c}, \Omega^* = \frac{\Omega c}{a}, J^* = \frac{J}{a^2}, \theta = \frac{T - T_0}{T_1 - T_0}, \phi^* = \frac{\phi - \phi_0}{\phi_1 - \phi_0} \quad (8)$$

Using equation (8) and dropping the star mark, we get the non dimensional form of equations (3-7) as:

$$Re \delta \left[ u \frac{\partial u}{\partial x} + v \frac{\partial u}{\partial y} \right] = -\frac{\partial p}{\partial x} + \frac{k}{\mu} \frac{\partial \Omega}{\partial y} + \frac{k + \mu}{\mu} \left[ \delta^2 \frac{\partial^2 u}{\partial x^2} + \frac{\partial^2 u}{\partial y^2} \right] - \left( \frac{a^2}{k_i} + \frac{\sigma B_0^2 a^2}{\mu} \right) u \quad (9)$$

$$Re \delta^3 \left[ u \frac{\partial v}{\partial x} + v \frac{\partial v}{\partial y} \right] = -\frac{\partial p}{\partial y} + \delta^2 \frac{k}{\mu} \frac{\partial \Omega}{\partial x} + \delta^2 \frac{k + \mu}{\mu} \left[ \delta^2 \frac{\partial^2 v}{\partial x^2} + \frac{\partial^2 v}{\partial y^2} \right] - \delta^2 \frac{a^2}{k_i} v \quad (10)$$

$$Re \delta \frac{\mu J}{k} \left[ u \frac{\partial \Omega}{\partial x} + v \frac{\partial \Omega}{\partial y} \right] = -2\Omega + \left[ \delta^2 \frac{\partial v}{\partial x} - \frac{\partial u}{\partial y} \right] + \frac{\gamma_1}{a^2 k} \left[ \delta^2 \frac{\partial^2 \Omega}{\partial x^2} + \frac{\partial^2 \Omega}{\partial y^2} \right] \quad (11)$$

$$Re P_r \delta \left[ u \frac{\partial \theta}{\partial x} + v \frac{\partial \theta}{\partial y} \right] = \left[ \delta^2 \frac{\partial^2 \theta}{\partial x^2} + \frac{\partial^2 \theta}{\partial y^2} \right] - \gamma P_r \theta \quad (12)$$

$$\delta \left[ u \frac{\partial \varphi}{\partial x} + v \frac{\partial \varphi}{\partial y} \right] = \frac{1}{S_c} \left[ \delta^2 \frac{\partial^2 \varphi}{\partial x^2} + \frac{\partial^2 \varphi}{\partial y^2} \right] + S_r \left[ \delta^2 \frac{\partial^2 \theta}{\partial x^2} + \frac{\partial^2 \theta}{\partial y^2} \right] - S \varphi \quad (13)$$

For long wavelength (i.e.  $\delta \ll 1$ ) and low Reynolds number (i.e.  $Re \rightarrow 0$ ) the system of equations (9-13) can be reduced to:

$$\frac{1}{1-N} \frac{\partial^2 u}{\partial y^2} + \frac{N}{1-N} \frac{\partial \Omega}{\partial y} - n^2 u = \frac{\partial P}{\partial x} \quad (14)$$

$$\frac{\partial P}{\partial y} = 0 \quad (15)$$

$$\frac{2-N}{m^2} \frac{\partial^2 \Omega}{\partial y^2} - \frac{\partial u}{\partial y} - 2\Omega = 0 \quad (16)$$

$$\frac{\partial^2 \theta}{\partial y^2} - \gamma P_r \theta = 0 \quad (17)$$

$$\frac{1}{S_c} \frac{\partial^2 \varphi}{\partial y^2} + S_r \frac{\partial^2 \theta}{\partial y^2} - S \varphi = 0 \quad (18)$$

where  $N = \frac{k}{k + \mu}$  is the coupling number,  $n^2 = a_1^2 + M^2$ ,  $a_1^2 = \frac{\alpha^2}{k_1}$  is the porosity parameter,  $M^2 = \frac{\sigma B_0^2 a^2}{\mu}$  is

the magnetic parameter,  $m^2 = \frac{a^2 k (2\mu + k)}{\gamma_1 (\mu + k)}$  is the micropolar parameter,  $P_r = \frac{\mu c_p}{k}$  is the Prandtl number,

$S_c = \frac{\mu}{\rho D_m}$  is the Schmidt number,  $S_r = \frac{D_m k_r \rho (T_1 - T_0)}{T_m \mu (\varphi_1 - \varphi_0)}$  is the Soret number,  $Re = \frac{\rho c a}{\mu}$  is the Reynolds

number,  $\gamma = \frac{Q_0 a^2}{\mu c_p}$  is the coefficient of heat absorption and  $S = \frac{k_2 a}{c}$  is the coefficient of chemical reaction.

From equation (15), it is clear that  $P$  is independent of  $y$ . Therefore equation (14) can be written as:

$$\frac{\partial^2 u}{\partial y^2} - n^2 (1-N)u + N \frac{\partial \Omega}{\partial y} - (1-N) \frac{dP}{dx} = 0 \quad (19)$$

The dimensionless boundary conditions are:

$$\frac{\partial u}{\partial y} = 0, \frac{\partial \Omega}{\partial y} = 0, \theta = 0 \text{ and } \varphi = 0 \text{ at } y = 0 \quad (20)$$

$$u = -1, \Omega = 0, \theta = 1 \text{ and } \varphi = 1 \text{ at } y = h \quad (21)$$

Introducing the stream functions  $\psi$  such that:

$$u = \frac{\partial \psi}{\partial y}$$

Then equations (16) and (19) take the form:

$$\frac{\partial^2 \psi}{\partial y^2} - n^2 (1-N) \frac{\partial \psi}{\partial y} + N \frac{\partial \Omega}{\partial y} - p_1 = 0 \quad (22)$$

$$\frac{2-N}{m^2} \frac{\partial^2 \Omega}{\partial y^2} - \frac{\partial \psi}{\partial y} - 2\Omega = 0 \quad (23)$$

where  $p_1 = (1-N) \frac{dP}{dx}$

Using the condition  $\psi = 0$  at  $y = 0$ , the general solution of equations (17), (18) (22) and (23) by using the boundary conditions (20) and (21) are given by:

$$\psi = \frac{c_1 + 2P_1 y}{b_1} + e^{b_2 y} c_2 + e^{-b_2 y} c_3 + e^{b_2 y} c_4 + e^{-b_2 y} c_5 \quad (24)$$

$$u = \frac{2P_1}{b_1} + e^{b_2 y} b_2 c_2 - e^{-b_2 y} b_2 c_3 + e^{b_2 y} b_3 c_4 - e^{-b_2 y} b_3 c_5 + \frac{2P_1}{b_1} \quad (25)$$

$$\Omega = \frac{e^{-y(\frac{\sqrt{\alpha}}{\alpha} + b_2 + b_3)} \left( e^{y b_3} b_3 \left( e^{y b_2} \left( e^{\frac{2\sqrt{\alpha} y}{\alpha}} c_6 + c_7 \right) b_4 + e^{\frac{\sqrt{\alpha} y}{\alpha}} b_2^2 (e^{2y b_2} c_2 + c_3) \right) \right) + e^{y(\frac{\sqrt{\alpha}}{\alpha} + b_2 + 2b_3)} b_3^2 b_4 c_4 + e^{y(\frac{\sqrt{\alpha}}{\alpha} + b_2)} b_3^2 b_4 c_5}{b_4 b_3} \quad (26)$$

$$\theta = \frac{1}{2} e^{(h-y)\sqrt{\gamma}\sqrt{P_r}} \left( 1 + e^{2y\sqrt{\gamma}\sqrt{P_r}} \right) \left( -1 + \coth \left[ h\sqrt{\gamma}\sqrt{P_r} \right] \right) \quad (27)$$

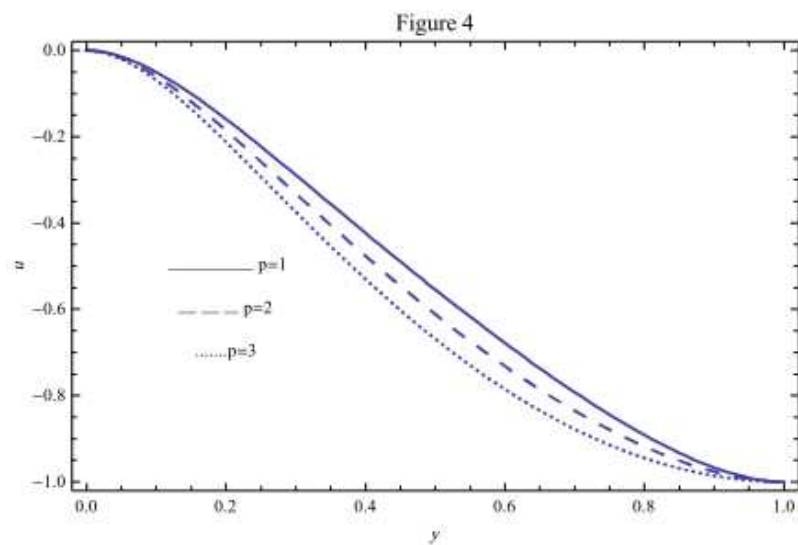
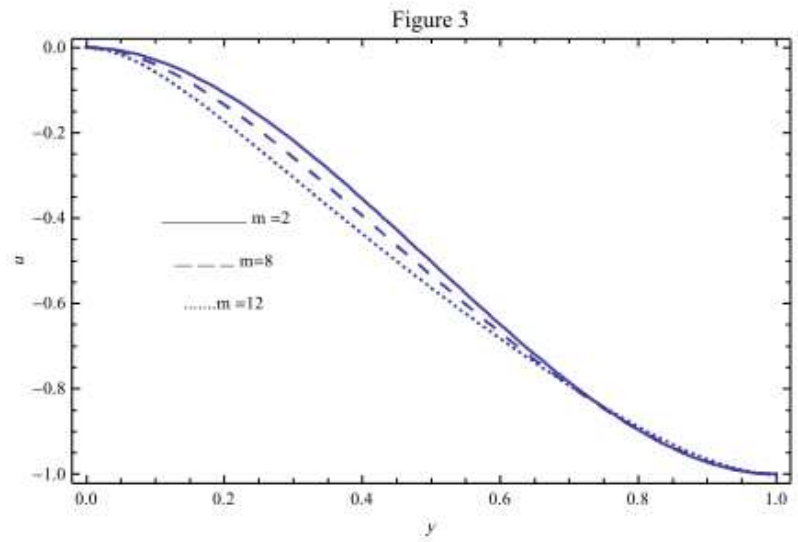
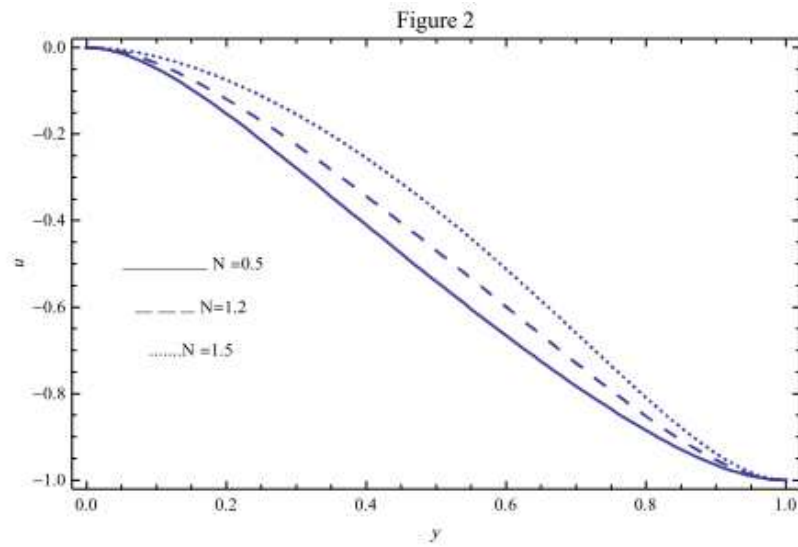
$$\varphi = \frac{y \text{Csch} \left[ h\sqrt{\gamma}\sqrt{P_r} \right] \sinh \left[ y\sqrt{\gamma}\sqrt{P_r} \right] P_r S_c S_r + \text{Csch} \left[ h\sqrt{S}\sqrt{S_c} \right] \text{Sinh} \left[ \sqrt{S} y \sqrt{S_c} \right] (SS_c - P_r (\gamma + \gamma S_c S_r))}{-\gamma P_r + SS_c} \quad (28)$$

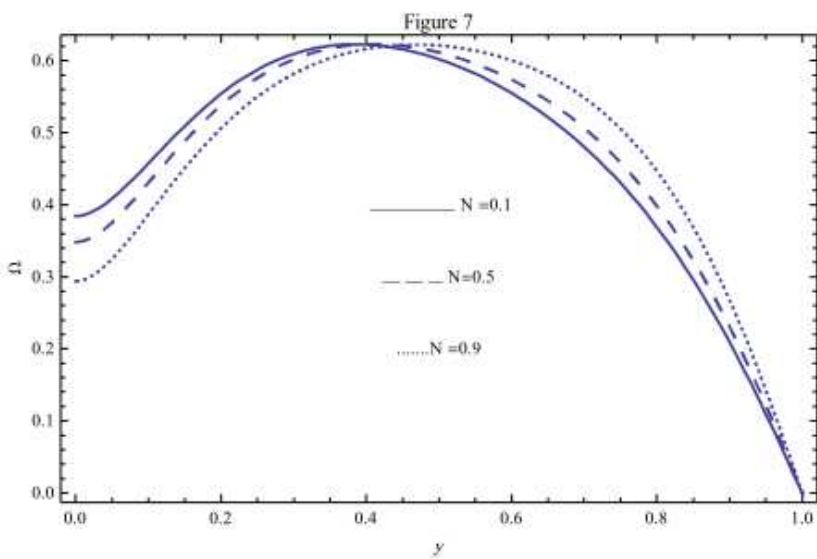
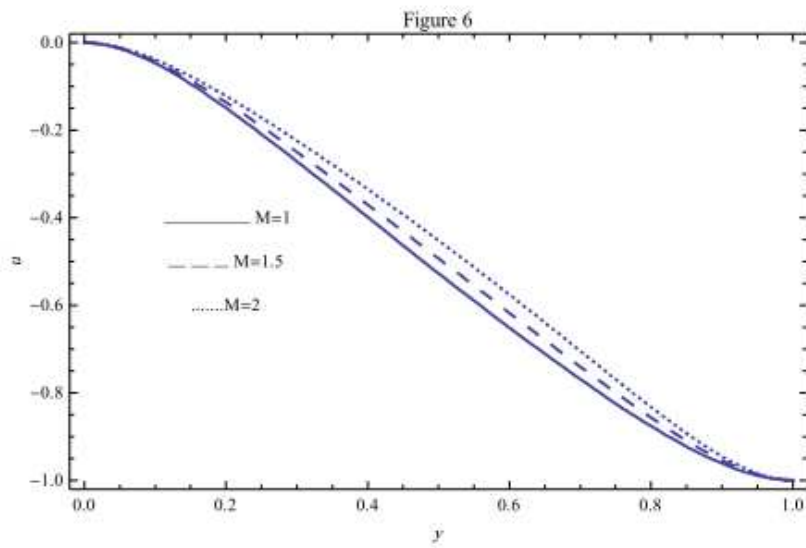
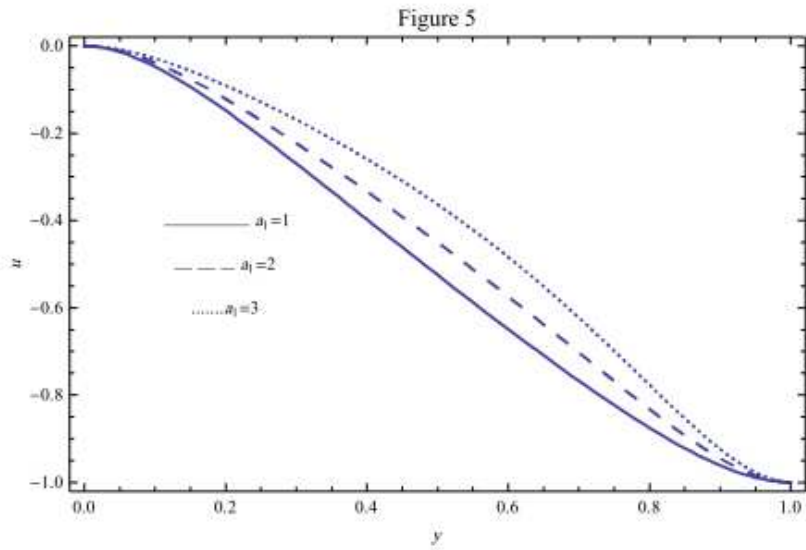
where  $c_1 \rightarrow c_7, b_1 \rightarrow b_5$  and  $\alpha$  are defined in the appendix.

## RESULTS AND DISCUSSION

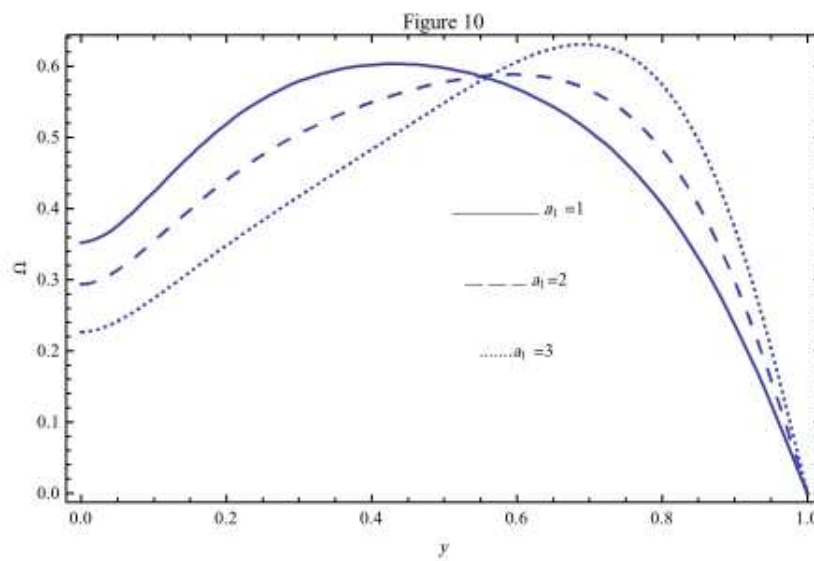
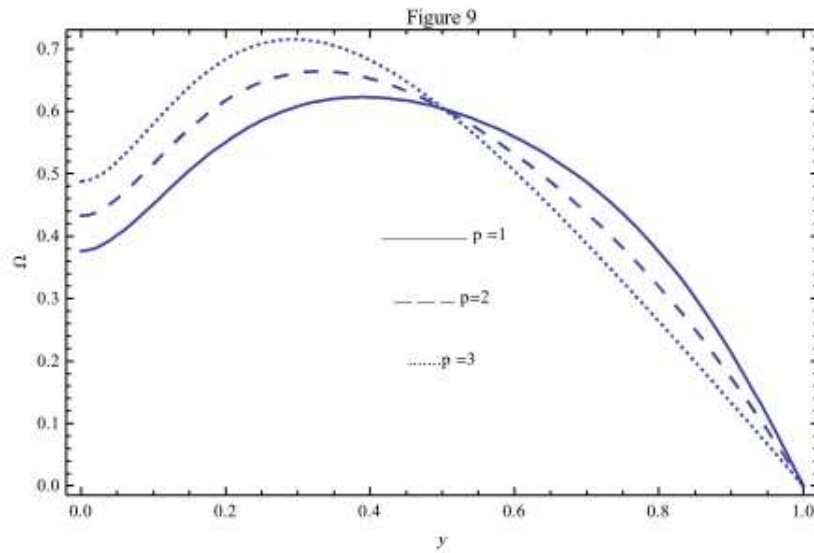
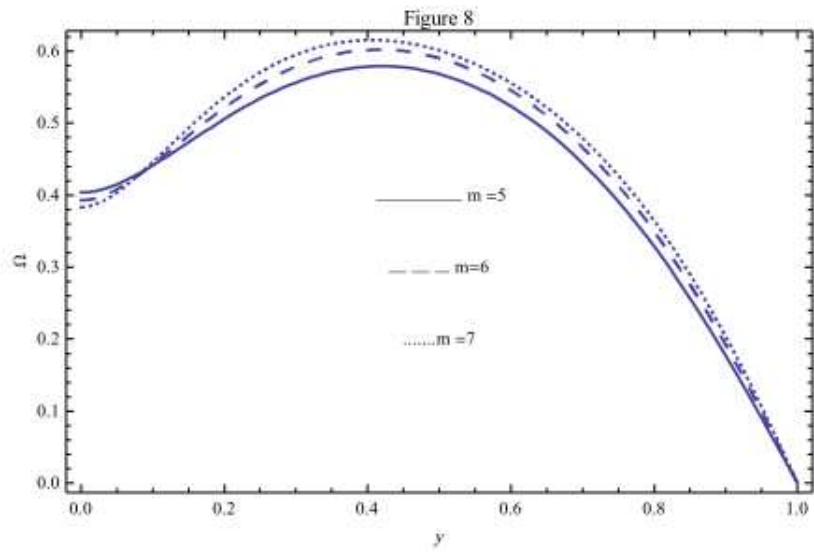
The peristaltic motion of a viscous incompressible micropolar fluid through a porous medium in a symmetric channel under the effects of heat absorption and chemical reaction in the presence of magnetic field has been considered in this paper. The resulting equations which control the motion of a micropolar fluid are solved by using the mathematical program in the case of long wavelength and low Reynolds number. The stream function, velocity, microrotation velocity, temperature and concentration of micropolar fluid are obtained. The effects of the pertinent parameters such as the coupling number  $N$ , the micropolar parameter  $m$ , the pressure  $P$ , the coefficient of heat absorption  $\gamma$ , the porosity parameter  $a_1$ , the coefficient of chemical reaction  $S$ , the Schmidt number  $S_c$ , Soret number  $S_r$  and the magnetic parameter  $M$  on these distributions are discussed by a set of graphs.

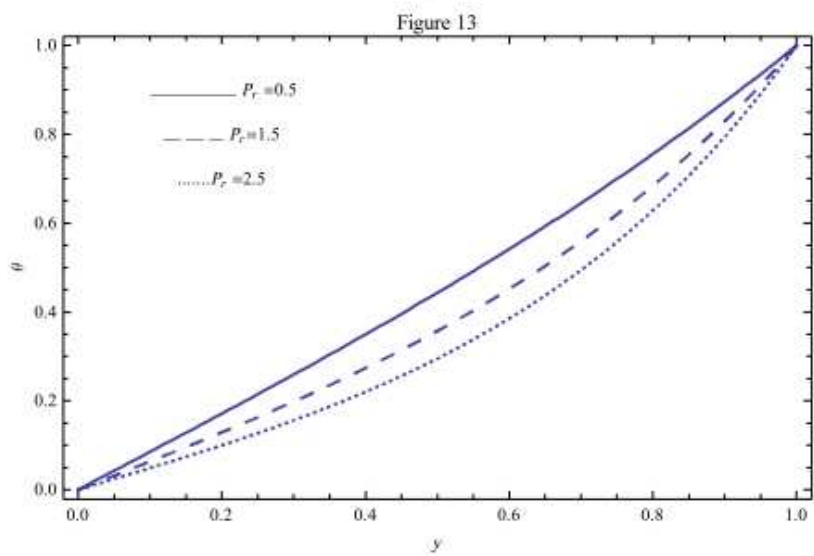
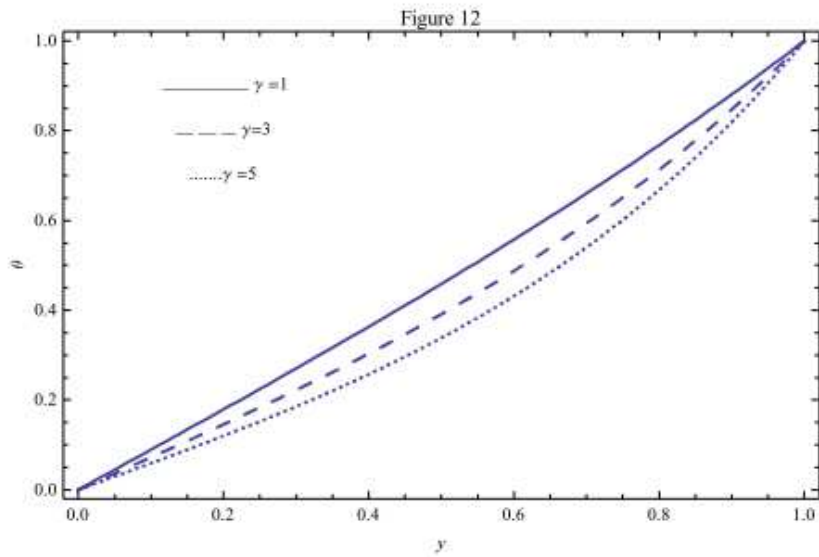
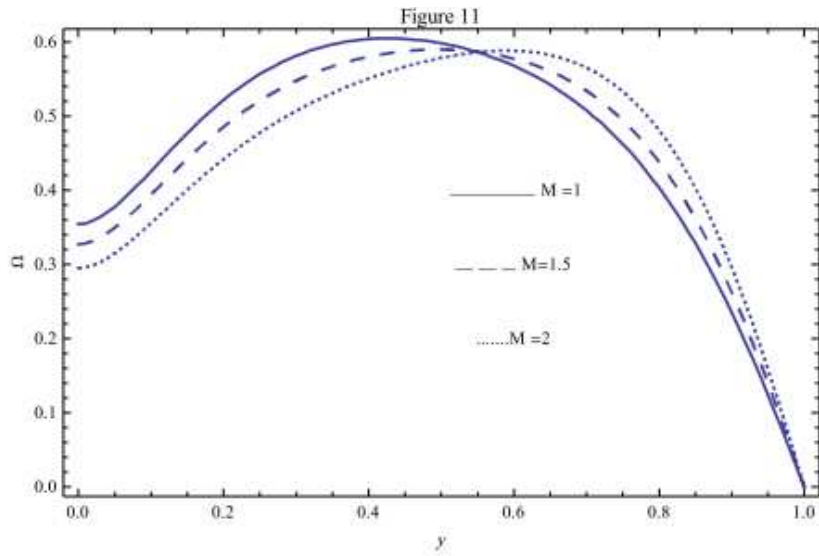
The effects of pertinent parameters on the velocity distribution are discussed through the figures (2-6). In these figures the velocity distribution  $u$  is plotted against the coordinate  $y$ . Figure (2) exhibits the effect of the coupling number  $N$ . It is found that the velocity increases with increasing  $N$ . The velocity at fixed values of  $y$  decreases with an increase in the micropolar parameter ( $m$ ) as shown in figs (3). It is seen from figure (4) that the velocity  $u$  decreases by increasing the pressure  $P$ . The effects of the porosity parameter  $a_1$  and the magnetic parameter  $M$  are shown graphically through the figures (5) and (6). In these figures it is observed that velocity  $u$  increases with the increase of  $a_1$  and  $M$ . Figures (7-11) exhibit the effects of the above parameters on the microrotation velocity  $\Omega$  is drawn against  $y$ . Figs (7) and (8) illustrate the effects of the coupling number  $N$  and the micropolar parameter  $m$ . It is seen that microrotation velocity  $\Omega$  at fixed values of  $y$  decreases as  $N$  and  $m$  increase, this occurs near the center and the inverse effect is observed near the upper wall. Figure (9) reveals that the effect of the pressure  $P$  on the microrotation velocity  $\Omega$ . It is seen that the microrotation velocity  $\Omega$  increases by increasing  $P$ , this occurs near the center and the inverse effect is marked near the upper wall. Figures (10) and (11) show the variation of the microrotation velocity  $\Omega$  for different values of the porosity parameter  $a_1$  and the magnetic parameter  $M$ . It is found that the microrotation velocity  $\Omega$  decreases with the increase in both  $a_1$  and  $M$ . This occurs near the center and the inverse effect occurs near the upper wall.

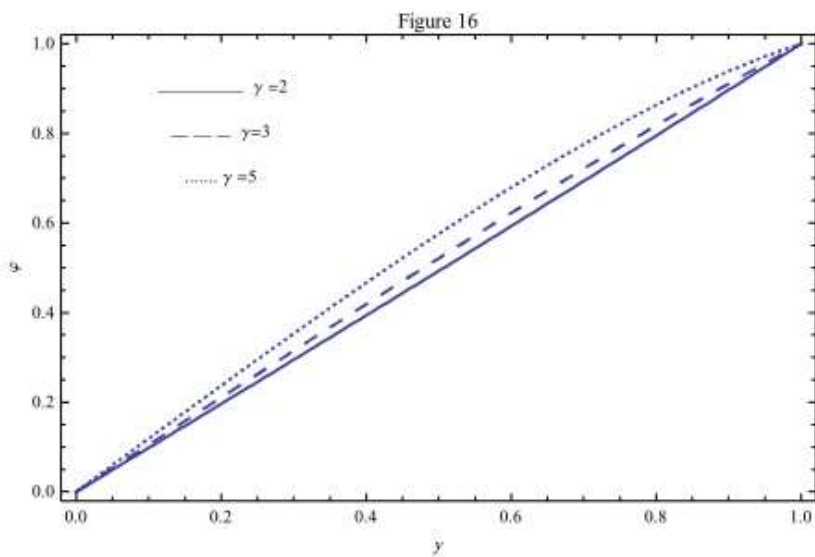
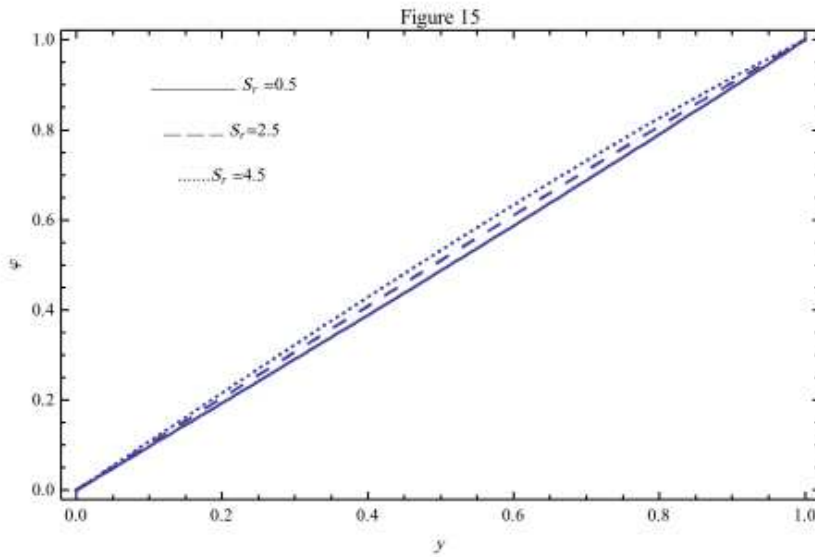
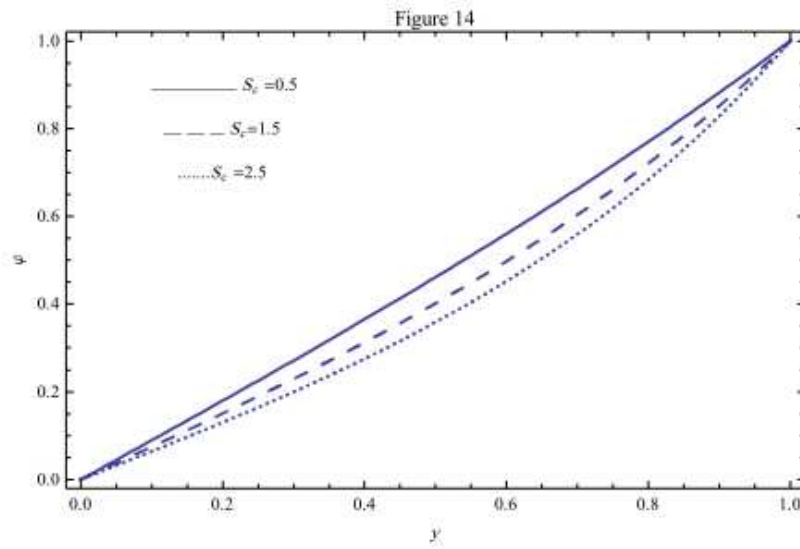


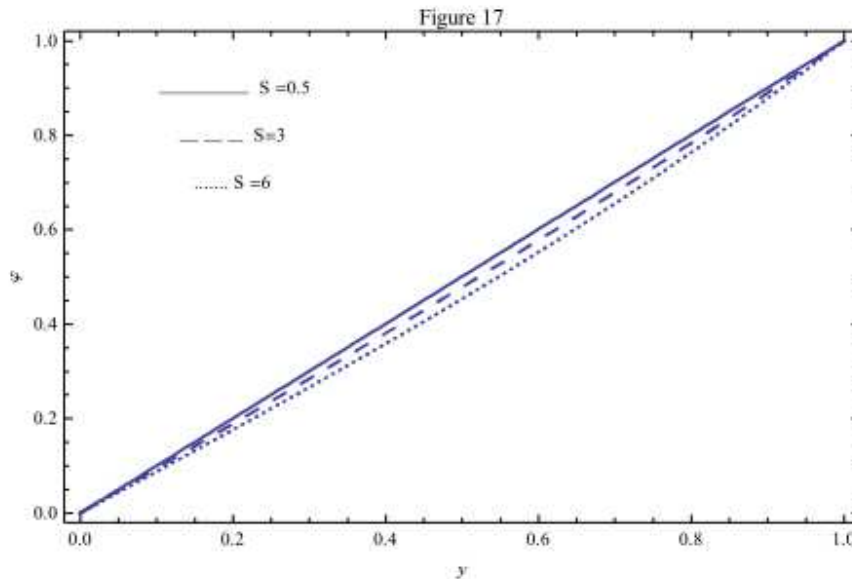












The effect of the different parameters on the temperature distribution when plotted against  $y$  is shown graphically through figures (12) and (13). In these figures the temperature  $\theta$  decreases by increasing the coefficient of heat absorption  $\gamma$  and the Prandtl number  $P_r$ . The Prandtl number  $P_r$  is a dimensional number approximating the ratio of kinematic viscosity (momentum diffusivity) and thermal diffusivity.

Figure (14) shows the effect of the Schmidt number  $S_c$  on the concentration  $\phi$  when plotted against  $y$ . It is clear that  $\phi$  decreases by increasing  $S_c$ . In figures (15) and (16) the concentration  $\phi$  increase by increasing Soret number  $S_r$  and the coefficient of heat absorption  $\gamma$ . Figure (17) represents the effect of the coefficient of chemical reaction  $S$  on the concentration  $\phi$ . It is observed that  $\phi$  decrease by increasing  $S$ .

**APPENDIX:**

$$c_1 = \frac{2(b_2^2 - b_3^2)(2e^{h(b_2+b_3)}b_1(\sinh[hb_2]b_2 - \sinh[hb_3]b_3) + (-1 + e^{hb_2})k_1(-1 - e^{hb_2})(-1 + e^{hb_3})b_2 + b_3k_1k_2)p_1}{b_2b_3(-2(1 + e^{2hb_2} + e^{2hb_3} - 4e^{h(b_2+b_3)} + e^{2h(b_2+b_3)})b_2b_3 + b_2^2k_5k_6 + b_3^2k_5k_6)}$$

$$c_2 = \frac{b_3(b_1(e^{hb_2} - 2e^{hb_3} + e^{h(b_2+2b_3)})b_2 - e^{hb_2}b_3k_6) + 2k_2((-1 - e^{hb_3})b_5k_1 + b_2k_2k_5)p_1}{b_1b_2(-2(1 + e^{2hb_2} + e^{2hb_3} - 4e^{h(b_2+b_3)} + e^{2h(b_2+b_3)})b_2b_3 + b_2^2k_5k_6 + b_3^2k_5k_6)}$$

$$c_3 = \frac{e^{hb_2}b_3(-b_1((1 + e^{2hb_3} - 2e^{h(b_2+b_3)})b_2 + b_3k_6) + 2(-1 - e^{hb_2})b_2k_2^2 + b_3k_1k_6)p_1}{b_1b_2(-2(1 + e^{2hb_2} + e^{2hb_3} - 4e^{h(b_2+b_3)} + e^{2h(b_2+b_3)})b_2b_3 + b_2^2k_5k_6 + b_3^2k_5k_6)}$$

$$c_4 = \frac{b_2(b_1((-2e^{hb_2} + e^{h(2b_2+b_3)})b_3 - e^{hb_3}b_2k_5) + 2k_1(-1 - e^{hb_2})b_2k_2 + b_3k_1k_4)p_1}{b_1b_2(-2(1 + e^{2hb_2} + e^{2hb_3} - 4e^{h(b_2+b_3)} + e^{2h(b_2+b_3)})b_2b_3 + b_2^2k_5k_6 + b_3^2k_5k_6)}$$

$$c_5 = \frac{e^{hb_3} b_2 \left( -b_1 \left( (1 + e^{2hb_2} - 2e^{h(b_2+b_3)}) b_3 + b_2 k_5 \right) + 2 \left( (-1 - e^{hb_3}) b_3 k_1^2 + b_2 k_2 k_5 \right) p_1 \right)}{b_1 b_2 \left( -2 \left( 1 + e^{2hb_2} + e^{2hb_3} - 4e^{h(b_2+b_3)} + e^{2h(b_2+b_3)} \right) b_2 b_3 + b_2^2 k_5 k_6 + b_3^2 k_5 k_6 \right)}$$

$$c_6 = \frac{1}{\sqrt{2} \left( 1 + e^{\frac{2\sqrt{2}h}{\alpha}} \right) (-2 + \alpha b_2^2) (-2 + \alpha b_3^2)} e^{-h(b_2+b_3)} \left( -e^{h(b_2+b_3)} \right) \sqrt{\alpha} b_2^3 (-2 + \alpha b_3^2) (c_2 - c_3) 2e^{hb_2} b_3^2 \sqrt{\alpha} b_3 (c_4 - c_5)$$

$$+ \sqrt{2} e^{\frac{\sqrt{2}h}{\alpha}} \left( e^{2hb_3} c_4 + c_5 \right) - b_2^2 \left( \sqrt{2} e^{h \left( \frac{\sqrt{2}}{\alpha} + 2b_2 + b_3 \right)} \right) (-2 + \alpha b_3^2) c_2 + \sqrt{2} e^{h \left( \frac{\sqrt{2}}{\alpha} + b_3 \right)} (-2 + \alpha b_3^2) c_3$$

$$+ e^{hb_2} \alpha b_3^2 \left( \sqrt{2} e^{\frac{\sqrt{2}h}{\alpha} + 2hb_3} c_4 + e^{hb_3} \sqrt{\alpha} b_3 (c_4 - c_5) + \sqrt{2} e^{\frac{\sqrt{2}h}{\alpha}} c_5 \right)$$

$$c_7 = \frac{1}{\sqrt{2} \left( 1 + e^{\frac{2\sqrt{2}h}{\alpha}} \right) (-2 + \alpha b_2^2) (-2 + \alpha b_3^2)} e^{-h(b_2+b_3)} \left( e^{h \left( \frac{2\sqrt{2}}{\alpha} b_2 + b_3 \right)} \right) \sqrt{\alpha} b_2^3 (-2 + \alpha b_3^2) (c_2 - c_3)$$

$$+ 2e^{h \left( \frac{\sqrt{2}}{\alpha} + b_2 \right)} b_3^2 \left( -e^{h \left( \frac{\sqrt{2}}{\alpha} + b_3 \right)} \sqrt{\alpha} b_3 (c_4 - c_5) + \sqrt{2} \left( e^{2hb_3} c_4 + c_5 \right) \right) - e^{\frac{\sqrt{2}h}{\alpha}} b_2^2 \left( -e^{h \left( \frac{\sqrt{2}}{\alpha} + b_2 + b_3 \right)} \alpha^{3/2} b_3^3 (c_4 - c_5) \right)$$

$$+ \sqrt{2} \left( e^{h(2b_2+b_3)} \right) (-2 + \alpha b_3^2) c_2 + e^{hb_3} (-2 + \alpha b_3^2) c_3 + e^{hb_2} \alpha b_3^2 \left( e^{2hb_3} c_4 + c_5 \right)$$

$$b_1 = 2(-1+a)n^2$$

$$b_2 = \sqrt{\left( -\frac{m^2}{-2+N} + \frac{Nm^2}{2(-2+N)} - \frac{n^2}{-2+N} + \frac{3Nm^2}{2(-2+N)} - \frac{N^2 n^2}{2(-2+N)} - \frac{\sqrt{(2m^2 - Nm^2 + 2n^2 - 3Nm^2 + N^2 n^2)^2 - 4(-2+N)(-2m^2 n^2 + 2Nm^2 n^2)}}{2(-2+N)} \right)}$$

$$b_3 = \sqrt{\left( -\frac{m^2}{-2+N} + \frac{Nm^2}{2(-2+N)} - \frac{n^2}{-2+N} + \frac{3Nm^2}{2(-2+N)} - \frac{N^2 n^2}{2(-2+N)} - \frac{\sqrt{(2m^2 - Nm^2 + 2n^2 - 3Nm^2 + N^2 n^2)^2 - 4(-2+N)(-2m^2 n^2 + 2Nm^2 n^2)}}{2(-2+N)} \right)}$$

$$b_4 = -2 + \alpha b_2^2, b_5 = -2 + \alpha b_3^2, \alpha = \frac{2 - N}{m^2}$$

$$k_1 = -1 + e^{hb_2}, k_2 = -1 + e^{hb_3}, k_3 = 1 + e^{hb_2}, k_4 = 1 + e^{hb_3}, k_5 = -1 + e^{2hb_2}, k_6 = -1 + e^{2hb_3}$$

**CAPTION OF FIGURES:**

Fig.2 The velocity distribution  $u$  is plotted against  $y$  for different values of  $N$  when  $m = 8, p = 1, a_1 = 0.1, M = 0.3, \epsilon = 0.5, x = \pi, t = \pi$ .

Fig.3 The velocity distribution  $u$  is plotted against  $y$  for different values of  $m$  when  $N = 0.2, p = 1, a_1 = 0.1, M = 0.3, \epsilon = 0.5, x = \pi, t = \pi$ .

Fig.4 The velocity distribution  $u$  is plotted against  $y$  for different values of  $P$  when  $m = 8, N = 0.2, a_1 = 0.1, M = 0.3, \epsilon = 0.5, x = \pi, t = \pi$ .

Fig.5 The velocity distribution  $u$  is plotted against  $y$  for different values of  $a_1$  when  $m = 8, N = 0.2, p = 1, M = 0.3, \epsilon = 0.5, x = \pi, t = \pi$ .

Fig.6 The velocity distribution  $u$  is plotted against  $y$  for different values of  $M$  when  $m = 8, N = 0.2, p = 1, a_1 = 0.1, \epsilon = 0.5, x = \pi, t = \pi$ .

Fig.7 The microrotation velocity  $\Omega$  is plotted against  $y$  for different values of  $N$  when  $m = 8, p = 1, a_1 = 0.1, M = 0.3, \epsilon = 0.5, x = \pi, t = \pi$ .

Fig.8 The microrotation velocity  $\Omega$  is plotted against  $y$  for different values of  $m$  when  $N = 0.2, p = 1, a_1 = 0.1, M = 0.3, \varepsilon = 0.5, x = \pi, t = \pi$ .

Fig.9 The microrotation velocity  $\Omega$  is plotted against  $y$  for different values of  $p$  when  $m = 8, N = 0.2, a_1 = 0.1, M = 0.3, \varepsilon = 0.5, x = \pi, t = \pi$ .

Fig.10 The microrotation velocity  $\Omega$  is plotted against  $y$  for different values of  $a_1$  when  $m = 8, N = 0.2, p = 1, M = 0.3, \varepsilon = 0.5, x = \pi, t = \pi$ .

Fig.11 The microrotation velocity  $\Omega$  is plotted against  $y$  for different values of  $M$  when  $m = 8, N = 0.2, p = 1, a_1 = 0.1, \varepsilon = 0.5, x = \pi, t = \pi$ .

Fig.12 The temperature  $\theta$  is plotted against  $y$  for different values of  $\gamma$  when  $P_r = .71, \varepsilon = 0.5, x = \pi, t = \pi$ .

Fig.13 The temperature  $\theta$  is plotted against  $y$  for different values of  $P_r$  when  $\varepsilon = 0.5, x = \pi, t = \pi, \gamma = 0.5$ .

Fig.14 The concentration  $\phi$  is plotted against  $y$  for different values of  $S_c$  when  $\gamma = 2, S_r = 0.5, S = 2$

Fig.15 The concentration  $\phi$  is plotted against  $y$  for different values of  $S_r$  when  $\gamma = 2, S_c = 0.5, S = 2$ .

Fig.16 The concentration  $\phi$  is plotted against  $y$  for different values of  $\gamma$  when  $S_r = 0.5, S_c = 0.5, S = 2$

Fig.17 The concentration  $\phi$  is plotted against  $y$  for different values of  $S$  when  $S_r = 0.5, S_c = 0.5, \gamma = 2$

## CONCLUSION

- (i) It is concluded that the micropolar parameters, magnetic parameter, gravity parameter and permeability have a deep effect on the onset of the convection in porous medium.
- (ii) Both the linear velocity and microrotation velocity decrease with increasing values of the micropolar parameter.
- (iii) It is found that the porosity parameter and magnetic parameter decelerate the microrotation velocity and accelerate the linear velocity.
- (iv) The linear velocity and microrotation velocity have opposite effect with increasing values of coupled number and pressure.
- (v) The temperature decreases with increasing values of the coefficient of heat absorption and Prandtl number.
- (vi) The concentration decreases with an increase of Schmidt number and chemical reaction parameter but the opposite effect is observed in case of Soret number and heat absorption parameter.
- (vii) It is observed that the coefficient of heat absorption has opposite effect on temperature distribution and concentration distribution.

## REFERENCES

- [1] Kavitha A, Reddy R, Sreenadh S, Saravana R, Srinivas A, *Advances in Applied Science Research*, **2011**, 1, 269-279.
- [2] Muthu P, Rathish B, Chandra P, *Applied Mathematical Modeling*, **2008**, 32 2019-2033.
- [3] Sreenadh S, Lakshminarayana P, Sucharitha G, *Int. J. of Appl. Math. Mech*, **2011**, 20 18-37.
- [4] Muthu P, Rathish B, Chandra P, *Anziam J.*, **2003**, 45, 245-260.
- [5] Mekheimer Kh,S, *Arabian Journal for Science and Engineering A*, **2003**, 28 (2), 183–201.
- [6] Elshehawey EF, Eldabe NT, Elghazy EM, and Ebaid A, *Applied Mathematics and Computation*, **2006**, 182 (1), 140–150.
- [7] Abd Elmaboud Y, *Journal of Porous Media*, **2011**, 14 (11), 1033–1045.
- [8] El-dabe NT, Kamel KA, Galila abd-Allah M, and Ramadan SF, *The African Journal of Mathematics and Computer Science Research*, **2013**, 6 (5), 94–101.
- [9] Muthu P, Rathish Kumar BV, and Chandra P, *Applied Mathematical Modelling*, **2008**, 32 (10), 2019–2033.
- [10] Reddy GR, Narayana PVS, and Venkataramana S, *Applied Mathematical Sciences*, **2010**, 4 (35), 1729–1741.
- [11] Ali N, Hayat T *Computers and Mathematics with applications*, **2008**, 55 (4), 589-608.
- [12] Muthu P, Rathish Kumar BV, Chandra P *Applied Mathematical Modelling*, **2008**, 32, 2019-2033.
- [13] Sreenadh S, Lakshminarayana P, Sucharitha G *Int. J. of Appl. Math. and Mech*, **2011**, 7 (20), 18-37.

- 
- [14] Harish Babu D, Satya Narayana PV “ Influence of variable permeability and radiation absorption on heat and mass transfer in MHD micropolar flow over a vertical moving porous plate,” *Hindawi Publishing Corporation ISRN Thermodynamics*, **2013**, Vol. 2013, Article ID 953536, 17 pages.
- [15] Hayat T, Khan M, Asghar S, Siddiqui AM, *J. Porous Media*, **2006**, 9, 55–67.
- [16] Mishra M, Rao AR, *Z. Angew. Math. Phys*, **2004**, 54, 532–550.
- [17] Reddy R, Kavitha A, Sreenadh S, Hariprabakran P, *International Journal of Innovative Technology and Engineering*, **2012**, 6, 22-29.
- [18] Afifi N, Mahmoud S, Al-Isede H, *International Mathematical Forum*, **2011**, 27, 1345-1356.
- [19] Vasudev C, Rajeswara U, Prabhakara G, Subba M, *Int. J. Cur. Sci. Res.*, **2011**, 3, 105-110.
- [20] El-Sayed M, El-Dabe N, Ghaly A, *Transp Porous Med*, **2011**, 89, 185-212.
- [21] Jothi S, Ramakrishna Prasad A, Reddy MV Subba *Adv. Appl. Sci. Res*, **2012**, 3(4), 2108-2119.
- [22] Akbar NS, Nadeem S, Lee C, *Int. J. Phys. Sci.*, **2012**, 7, 687.
- [23] Pandey SK, Chaube MK, *Commun. Nonlinear Sci. Numer. Simulat.*, **2011**, 16, 3591.
- [24] Nabil T. M. Eldabe Nabil TM, Bothaina M. Agoor, Heba Alame, *Journal of Fluids*, **2014**, Vol.2014, Article ID 525769, 12 pages.
- [25] Eldabe N, Mohamed A, *Arabian Journal For Science and Engineering*, **2014**, 39 (6), 5045.